HHS Public Access

Author manuscript

J Am Chem Soc. Author manuscript; available in PMC 2018 September 13.

Published in final edited form as:

J Am Chem Soc. 2017 September 13; 139(36): 12410–12413. doi:10.1021/jacs.7b07485.

Facile Assembly/Disassembly of DNA Nanostructures Anchored on Cell-Mimicking Giant Vesicles

Ruizi Peng[†], **Huijing Wang**[†], **Yifan Lyu**[†,‡], **Liujun Xu**[†], **Hui Liu**[†], **Hailan Kuai**[†], **Qiaoling Liu**[†,*], and **Weihong Tan**[†,‡,*]

[†]Molecular Science and Biomedicine Laboratory, State Key Laboratory of Chemo/Bio-Sensing and Chemometrics, College of Chemistry and Chemical Engineering, College of Life Sciences, and Aptamer Engineering Center of Hunan Province, Hunan University, Changsha, Hunan 410082, China

[‡]Department of Chemistry and Department of Physiology and Functional Genomics, Center for Research at the Bio/Nano Interface, Health Cancer Center, UF Genetics Institute, McKnight Brain Institute, University of Florida, Gainesville, Florida 32611-7200, United States

Abstract

DNA nanostructures assembled on living cell membranes have become powerful research tools. Synthetic lipid membranes have been used as a membrane model to study the dynamic behavior of DNA nanostructures on fluid soft lipid bilayers, but without the inherent complexity of natural membranes. Herein, we report the assembly and disassembly of DNA nanoprisms on cell-mimicking micrometer-scale giant membrane vesicles derived from living mammalian cells. Three-dimensional DNA nanoprisms with a DNA arm and a cholesterol anchor were efficiently localized on the membrane surface. The assembly and disassembly of DNA nanoprisms were dynamically manipulated by DNA strand hybridization and toehold-mediated strand displacement. Furthermore, the heterogeneity of reversible assembly/disassembly of DNA nanoprisms was monitored by Förster resonance energy transfer. This study suggests the feasibility of DNA-mediated functional biomolecular assembly on cell membranes for biomimetics studies and delivery systems.

Oligonucleotides have emerged as programmable building blocks to create dynamic molecular devices[1] from built-in DNA nanostructures.[2–4] These dynamic DNA functional units exhibit good performance and have been used in the construction of DNA walkers,[5] tweezers,[6] logic circuits,[7–9] gene regulators[10–12] and smart therapeutics.[13,14] Most recently, bioengineering has focused on DNA nanostructures on the cell surface, resulting in the

[*]Corresponding Authors: tan@chem.ufl.edu, qlliu@iccas.ac.cn.

ORCID

Qiaoling Liu: 0000-0001-9487-0944

Weihong Tan: 0000-0002-8066-1524

Notes

The authors declare no competing financial interest.

Supporting Information

The Supporting Information is available free of charge on the ACS Publications website at DOI: 10.1021/jacs.7b07485.

Additional information as noted in text (PDF)

design of many nanostructures and devices interacting with the cell membrane.[15] Hence, most such DNA nanostructures built on synthetic lipid membranes have served as biomimetic membrane proteins, such as ion channels,[16,17] membrane-sculpting protein[18] and “SNAP (Soluble NSF Attachment Protein) REceptor” (SNARE) protein.[19] To further manipulate DNA nanostructures at the mesoscale, strategies combining dynamic DNA nanotechnologies have been developed to study the complexities of cell membranes, such as cell-surface recognition[20,21] and membrane receptor studies.[22] However, such studies with DNA nano-structures are often confounded by dynamic cell behavior, observed, for example, in internalization and “flip-flop” leaflet movements.[23] To solve this problem, researchers have turned to fluid soft lipid bilayers as materials to build an ideal model for cell-surface studies of DNA nanostructures.

To date, different studies have reported the dynamic behavior of tethered DNA nanostructures on various lipid membranes.[24,25] However, all of these strategies have overlooked an obvious, but powerful, obstacle to the cell-mimicking membrane environment. As we know, membrane physico-chemical properties have a significant impact in dynamic behavior of DNA nanostructures and their assemblies.[26–29] This means that DNA nanostructures on these synthetic model membranes would be remarkably different from their dynamic behavior on the natural membrane.[30] Thus, it is necessary to study the dynamic behavior of DNA nanostructures on cell-mimicking giant vesicles model which would further advance our understanding on behavior of DNA nanostructures on biological interfaces.

Recently, giant membrane vesciles derived from live cells was proved to be an idea cell/membrane model. Because of their highly similarity to cell membrane structure, these membrane vesicles possess the unique superiority on a broad spectrum of studies such as biomembrane physics and biomimetic chemistry, such as phase separation and functional lipid raft domains, as well as membrane protein interactions.[31–33] However, the assembly of DNA nanostructures in such cell-mimicking giant membrane vesicles has not been carried out, even though they have been proved to be an idea platform as cell membrane model.

Herein, as a proof-of-concept, we report manipulating the assembly/disassembly of 3D DNA nanostructures on the cell-mimicking surfaces of micrometer-scale giant membrane vesicles (MVs). DNA triangular prisms (TPs) were selected as a feasible and efficient 3D DNA nanostructural model to study their dynamic behavior on lipid membrane.[34] Utilizing DNA hybridization and DNA strand displacement reaction, the dynamic assembly/disassembly processes of TPs on the MVs surface were studied, followed the monitoring by Förster resonance energy transfer (FRET) between the fluorophore pairs, and results also indicated the heterogeneity of DNA assembly on MVs.

As a starting point, a box-like nanoprism scaffold was initially fabricated by three long single-stranded DNAs (ssDNA) after annealing.[34,35] Because of 3D DNA nanostructures consists of at least three DNA strands, DNA TPs scaffolds can be created with the minimum number of DNA strands to meet the requirement of economy in the use of DNA materials. One ssDNA segment elongates from its top face, farthest from the vesicle surface, and serves as an arm (arm strand), whereas a cholesterol-labeled ssDNA segment elongates from

its bottom face, as an anchor (anchor strand) (Figure 1B) in order to immoblize the DNA nanoprism onto the surface of MVs. This nanoprism binds to the surface via hydrophobic cholesterol anchorage to the lipid bilayer of MVs, thus facilitating DNA-mediated dynamic regulation of the functional nanoprisms on the cell-mimicking membrane. Initially, we employed the native polyacrylamide gel electrophoresis (N-PAGE) to confirm the formation of the nanoprism scaffold in buffer solution (see Supporting Information (SI), Figure S1). Then the 3D DNA scaffold was transformed into a functional unit by loading an arm and an anchor strand (Figure 1B and SI, Figure S2).

After successfully demonstrating the feasibility of constructing these 3D DNA nanostructures, we investigated their plasticity in terms of ready assembly and disassembly. To accomplish this, The assembly/disassembly process of DNA nanoprisms was studied in buffer solution to verify their capacity for dynamic reversible manipulation (Figure 1A). Two different DNA nanostructures, TP-A and TP-B, were first constructed by loading alternative Arm A and Arm B strands on the top face, respectively. Assembly of TP-A and TP-B was achieved by hybridizing with a DNA linker. The optimized experiment also showed the high assembly efficiency of DNA nanoprisms (SI, Figure S3A,C). Then, to disassemble the dimeric DNA nanoprism, a toehold-mediated DNA strand displacement reaction was induced by a displacement strand, the disassembly efficiency was also optimozed (SI, Figure S3B,D). Next, N-PAGE results verified the dynamic assembly/disassembly process of TP-A and TP-B achieved by DNA hybridization and DNA strand displacement reaction (Figure 1C). Fluorescence spectral and kinetics results also demonstrated this efficient reversible manipulation, which in agreement with the gel electrophoresis results (SI, Figure S4).

Different from DNA nanoprisms assembled in buffer solution, where DNA strands are able to diffuse freely, the kinetics of DNA nanostructures on the surface of cell-mimicking giant vesicles was expected to be much more complex because they were derived from living cells and contain cell membrane constituents, such as proteins and glycocalyx,[30] likely impacting the kinetics of assembly and disassembly.

Previously, we developed a facile strategy to prepare micrometer-scale giant membrane vesicles.[36] They showed excellent cell-mimicking properties, thus providing an ideal dynamic soft platform at the mesoscale to study the behavior and kinetics of DNA nanostructures. Herein, cell-mimicking MVs detached from HeLa cells were initially obtained with good quality and high yields. To confirm the successful insertion of DNA nanostructures on the biological surface, multicolor fluorescence colocalization of nanoprisms was observed. First, three different DNA-fluorophore sequences were assembled with two nanoprism scaffolds in the test tube, in which a cholesterol-DNA-Alexa Fluor 488 sequence (AF 488-labeled anchor strand) was loaded on the bottom face of all nanoprisms. Afterward, fluorophore-modified nanoprisms TP-Cy3 and TP-Cy5 were created, in which Cy3- and Cy5-labeled arm strands were loaded on each respective top face.

To anchor nanoprisms on MVs, 22.2 μL mixtures of 9 μM cholesterol-labeled TP-Cy3 and TP-Cy5 were added to 400 μL MVs with 1640 medium containing 5 mM Mg^{2+}. The divalent cation contributes to the binding of DNA nanostructures to the negatively charged

lipid bilayers,[37] and it also maintains the stability and integrity of DNA nanostructures.[15] After incubation with MVs at 37 °C for 30 min, laser confocal scanning microscopy (LCSM) was employed to verify that the modified nanoprisms were readily localized on the cell-mimicking membrane of MVs in Group 1 (Figure 2A, the first panel), followed by quantification of fluorescence colocalization (SI, Figure S5). In the absence of DNA scaffolds, the anchor strand could immobilize onto the membrane via cholesterol insertion (Group 2), while the arm strands without cholesterol mainly distributed outside of the giant vesicles (Group 3). This result demonstrated that DNA TPs could bind to the lipid bilayer though cholesterol insertion, thus providing a facile strategy for anchoring DNA nanostructures to our cell-mimicking giant vesicles (SI, Figure S6). Moreover, the fluorescence intensity of the overlay images (488+Cy3+Cy5, Figure 2A, last line) was measured (Figure 2B) and also demonstrated that these DNA nanostructures could successfully anchor onto the membrane of MVs. Although the preference of DNA nanoprisms localized on the surface of MVs promised their reversible assembly and disassembly, synthetic giant vesicles made from phospholipid was not an idea platform for the surface manipulation, since nanoprisms are easily enriched in the chamber of MVs (SI, Figure S7). It indicate the behavior of DNA nanostructures on synthetic model membranes would be remarkably different from theirs on cell-mimicking surface.

To characterize the assembly/disassembly of cholesterol-labeled nanoprisms on the cell-mimicking membrane of MVs, we used a FRET configuration composed of TP-Cy3 and TP-Cy5. Thus, the dynamic assembly/disassembly of nanoprisms on the MVs could be visualized via the changes of FRET efficiency between Cy3 and Cy5 fluorescent dyes (Figure 3A). Initially, these nanoprisms (TP-Cy3: TP-Cy5 = 1:1.2) were mixed with MVs in solution and incubated at 37 °C for 10 min (panel 1). The assembly of TP-Cy3 and TP-Cy5 was performed by adding 1.5-fold excess DNA linker and incubating for 50 min at 4 °C (panel 2). Interestingly, we found that low temperature favored the assembly of TP-Cy3 and TP-Cy5 compared to 37 °C (SI, Figure S8), possibly due to the formation of a liquid-order phase in the lipid membrane.[38] We speculated that the cholesterol component of anchor strands prefers to exist in this phase, which may increase the opportunity for molecular collision and thus facilitate the assembly of nanoprisms. To monitor the disassembly, 2-fold excess displacement strand was added into solution of MVs and the mixture was incubated for another 1 h. As shown in panel 3, decreased FRET efficiency can be observed by separation of the Cy3- and Cy5-labeled nanoprisms on the cell-mimicking membrane driven by toehold-mediated DNA strand displacement. When a random strand was added to assemble TP-Cy3 with TP-Cy5 on the MVs surface, little effect could be detected, demonstrating that the assembly process was not driven by temperature, but rather by strand hybridization based on specific Watson–Crick DNA base pairing (Figure 3A, panel 4). Furthermore, quantitative assay of FRET efficiency between heteronanoprisms demonstrated the feasibility of nanoprism assembly/disassembly on the MVs surface (Figure 3B). More interestingly, DNA assembly on the MVs surface revealed heterogeneous FRET efficacy. The calculated ratiometric fluorescence from a randomly selected giant vesicle via acceptor photobleaching showed the heterogeneous FRET efficiency of dimeric nanoprism assembly on the surface of our giant vesicles (Figure 3C). Normally, lipid structure in a biomembrane (e.g., plasma membrane and organelle membrane) exists in the form of separated

microdomains, indicating the heterogeneity of the biomembrane.[38] The membrane of MVs derived from mammalian cells represents one such biomembrane. Thus, we speculated that our giant vesicles would also exhibit membrane heterogeneity and that the observed heterogeneous FRET efficiency was likely caused by localization of cholesterol-labeled nanoprisms in microdomains.

Along with developing nanotechnology, oligonucleotides not only play an important biological role in living systems but also have emerged as building blocks for self-assembly nano-fabrication. Here, the DNA nanoprism served as the simplest 3D DNA nanostructure model and was thought to find a wide applications in logic computation,[9] bioanalysis and biomimetics.[16] Besides this nanostructural aspect, the method is also generally applicable to other DNA nanostructures[37,39] based on Watson–Crick base pairing and the anchorage of hydrophobic components to membrane. Combining with cell-mimicking surface, manipution of these DNA nanofabrications provide a method to functionalize cell surface, which have to overcome dynamic cell surface movements, and suggest the long-term feasiblitity to regulate the membrane structures.

In summary, using DNA strand hybridization and toehold-mediated strand displacement, we have engineered the respective assembly and disassembly of DNA nanostructures on cell-mimicking membranes of MVs. The status of a single nanoprism and its dimeric assembly were monitored by FRET, and heterogeneous DNA assembly on MVs was observed. On the basis of the reported dynamic programmability, predictability and addressability of DNA nanostructures, the manipulation of membrane-anchored DNA nanostructures can serve as a new strategy for engineering artificial cells and combining DNA nanotechnology with biomimetics.

Supplementary Material

Refer to Web version on PubMed Central for supplementary material.

Acknowledgments

This work is supported by the China NSFC grants (NSFC 21502050, NSFC 21221003 and NSFC 21327009), and by the US National Institutes of Health (GM079359) and NSF 1645219.

References

1. Erbas-Cakmak S, Leigh DA, McTernan CT, Nussbaumer AL. Chem Rev. 2015; 115:10081–10206. [PubMed: 26346838]
2. Veneziano R, Ratanalert S, Zhang KM, Zhang F, Yan H, Chiu W, Bathe M. Science. 2016; 352:1534. [PubMed: 27229143]
3. Zhang F, Nangreave J, Liu Y, Yan H. J Am Chem Soc. 2014; 136:11198–11211. [PubMed: 25029570]
4. Chao J, Zhang YN, Zhu D, Liu B, Cui CJ, Su S, Fan CH, Wang LH. Sci China: Chem. 2016; 59:730–734.
5. You MX, Chen Y, Zhang XB, Liu HP, Wang RW, Wang KL, Williams KR, Tan WH. Angew Chem, Int Ed. 2012; 51:2457–2460.
6. Kemmerich FE, Swoboda M, Kauert DJ, Grieb MS, Hahn S, Schwarz FW, Seidel R, Schlierf M. Nano Lett. 2016; 16:381–386. [PubMed: 26632021]

7. Zhang DY, Hariadi RF, Choi HMT, Winfree E. Nat Commun. 2013; 4:1965. [PubMed: 23756381]
8. Dong YF, Dong C, Wan F, Yang J, Zhang C. Sci China: Chem. 2015; 58:1515–1523.
9. He KY, Li Y, Xiang BB, Zhao P, Hu YF, Huang Y, Li W, Nie Z, Yao SZ. Chem Sci. 2015; 6:3556–3564.
10. Benenson Y, Gil B, Ben-Dor U, Adar R, Shapiro E. Nature. 2004; 429:423–429. [PubMed: 15116117]
11. Zampini M, Mur LAJ, Stevens PR, Pachebat JA, Newbold CJ, Hayes F, Kingston-Smith A. Sci Rep. 2016; 6:26572. [PubMed: 27220405]
12. Elbaz J, Yin P, Voigt CA. Nat Commun. 2016; 7:11179. [PubMed: 27091073]
13. Douglas SM, Bachelet I, Church GM. Science. 2012; 335:831–834. [PubMed: 22344439]
14. Meng HM, Liu H, Kuai HL, Peng RZ, Mo LT, Zhang XB. Chem Soc Rev. 2016; 45:2583–2602. [PubMed: 26954935]
15. Chen YJ, Groves B, Muscat RA, Seelig G. Nat Nanotechnol. 2015; 10:748–760. [PubMed: 26329111]
16. Howorka S. Science. 2016; 352:890–891. [PubMed: 27199400]
17. Burns JR, Seifert A, Fertig N, Howorka S. Nat Nanotechnol. 2016; 11:152–156. [PubMed: 26751170]
18. Czogalla A, Kauert DJ, Franquelim HG, Uzunova V, Zhang YX, Seidel R, Schwille P. Angew Chem, Int Ed. 2015; 54:6501–6505.
19. Xu WM, Nathwani B, Lin CX, Wang J, Karatekin E, Pincet F, Shih W, Rothman JE. J Am Chem Soc. 2016; 138:4439–4447. [PubMed: 26938705]
20. You MX, Peng L, Shao N, Zhang LQ, Qiu LP, Cui C, Tan WH. J Am Chem Soc. 2014; 136:1256–1259. [PubMed: 24367989]
21. You MX, Zhu GZ, Chen T, Donovan MJ, Tan WH. J Am Chem Soc. 2015; 137:667–674. [PubMed: 25361164]
22. Chen Y, O'Donoghue MB, Huang YF, Kang HZ, Phillips JA, Chen XL, Estevez MC, Yang CYJ, Tan WH. J Am Chem Soc. 2010; 132:16559–16570. [PubMed: 21038856]
23. Klymchenko AS, Kreder R. Chem Biol. 2014; 21:97–113. [PubMed: 24361047]
24. Langecker M, Arnaut V, List J, Simmel FC. Acc Chem Res. 2014; 47:1807–1815. [PubMed: 24828105]
25. Suzuki Y, Endo M, Sugiyama H. ACS Nano. 2015; 9:3418–3420. [PubMed: 25880224]
26. Tan C, Terakawa T, Takada S. J Am Chem Soc. 2016; 138:8512–8522. [PubMed: 27309278]
27. Saleem M, Morlot S, Hohendahl A, Manzi J, Lenz M, Roux A. Nat Commun. 2015; 6:6249. [PubMed: 25695735]
28. Iversen L, Mathiasen S, Larsen JB, Stamou D. Nat Chem Biol. 2015; 11:822–825. [PubMed: 26485070]
29. Erlandson KJ, Bisht H, Weisberg AS, Hyun SI, Hansen BT, Fischer ER, Hinshaw JE, Moss B. Cell Rep. 2016; 14:2084–2091. [PubMed: 26923595]
30. Rode AB, Endoh T, Tateishi-Karimata H, Takahashi S, Sugimoto N. Chem Commun. 2013; 49:8444–8446.
31. Baumgart T, Hammond AT, Sengupta P, Hess ST, Holowka DA, Baird BA, Webb WW. Proc Natl Acad Sci U S A. 2007; 104:3165–3170. [PubMed: 17360623]
32. Levental I, Lingwood D, Grzybek M, Coskun U, Simons K. Proc Natl Acad Sci U S A. 2010; 107:22050–22054. [PubMed: 21131568]
33. Sarabipour S, Del Piccolo N, Hristova K. Acc Chem Res. 2015; 48:2262–2269. [PubMed: 26244699]
34. Conway JW, Madwar C, Edwardson TG, McLaughlin CK, Fahkoury J, Lennox RB, Sleiman HF. J Am Chem Soc. 2014; 136:12987–12997. [PubMed: 25140890]
35. Conway JW, McLaughlin CK, Castor KJ, Sleiman H. Chem Commun. 2013; 49:1172–1174.
36. Liu QL, Guan MR, Xu L, Shu CY, Jin C, Zheng JP, Fang XH, Yang YJ, Wang CR. Small. 2012; 8:2070–2077. [PubMed: 22508680]
37. Suzuki Y, Endo M, Sugiyama H. Nat Commun. 2015; 6:8052. [PubMed: 26310995]

38. Johnson SA, Stinson BM, Go MS, Carmona LM, Reminick JI, Fang X, Baumgart T. Biochim Biophys Acta, Biomembr. 2010; 1798:1427–1435.

39. Cutler JI, Auyeung E, Mirkin CA. J Am Chem Soc. 2012; 134:1376–1391. [PubMed: 22229439]

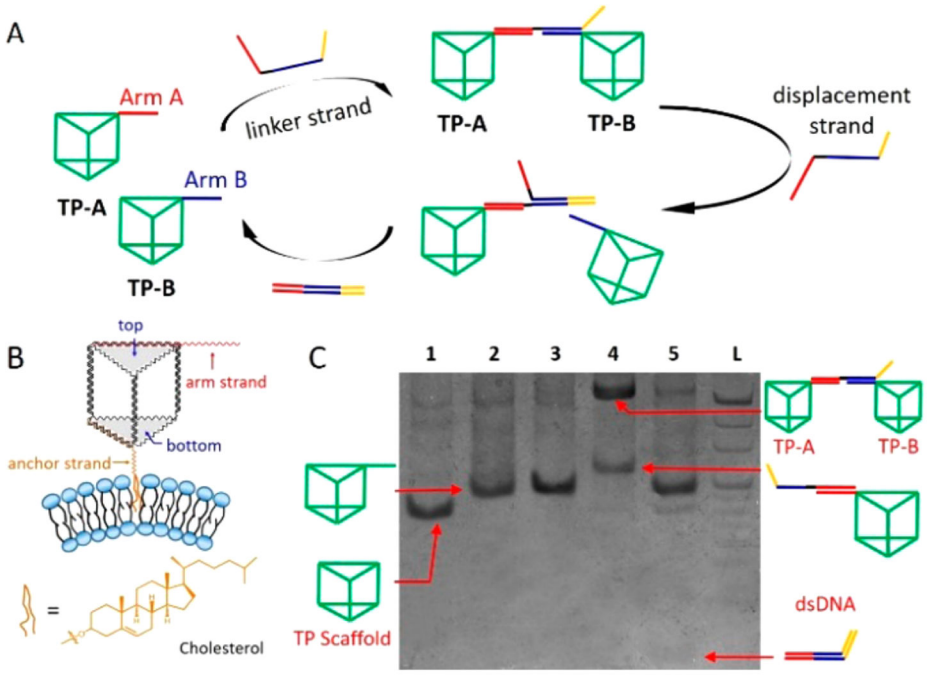

Figure 1.

Dynamic assembly/disassembly of DNA triangular nano-prism in reaction buffer. (A) Schematic representation of DNA-mediated assembly/disassembly of TP-A and TP-B by DNA hybridization and DNA strand displacement reaction. (B) Schematic representation of cholesterol-labeled DNA triangular nanoprism anchored on the bilayer of MVs. (C) Native polyacrylamide gel electrophoresis (5%) analysis of dynamic assembly/disassembly of DNA nanoprisms in reaction buffer. Lane 1: TP scaffold. Lane 2: TP-A. Lane 3: TP-B. Lane 4: hybridizing TP-A and TP-B by linker strand to assemble nanoprisms. Lane 5:1.2-fold excess displacement strand to disassemble the dimeric nanoprism. L: 20-bp ladder consisting of double strands of DNA with length increasing in 20-bp steps. All DNA bands were stained by Stains-All and then imaged using the Bio-Rad ChemiDoc XRS System.

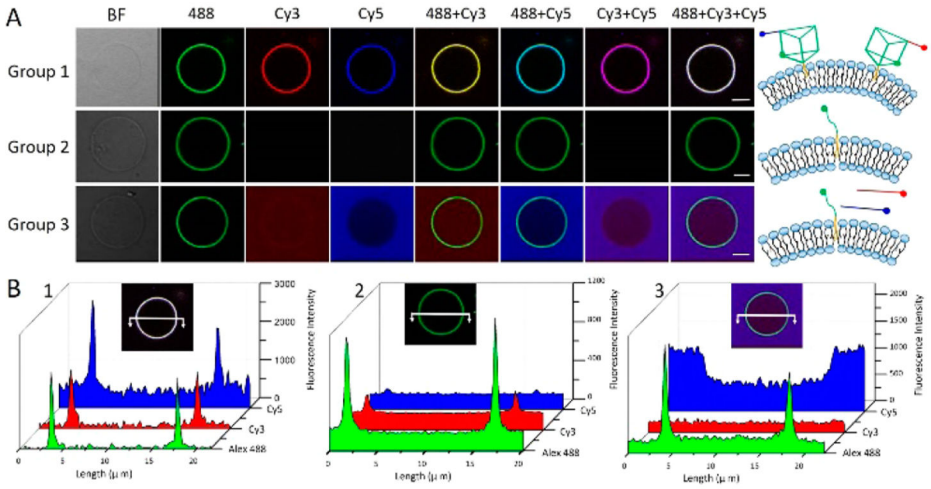

Figure 2.

Anchoring DNA nanoprisms on cell-mimicking giant vesicles. (A) Confocal laser scanning microscopy imaging of colocalization of 500 nM nanoprisms on MVs. Panel 1: TP-Cy3 and TP-Cy5 anchored on lipid bilayer through cholesterol-insertion. Panel 2: Single strand of Chol-DNA-Alexa Fluor 488. Panel 3: Single strand of Chol-DNA-Alexa Fluor 488 and free arm strands of Cy3-DNA and Cy5-DNA. All samples were incubated with 400 μL solution of MVs at 37 °C for 30 min. Scale Bar: 5 μm. (B) Cross section of fluorescence intensities (white solid line) in Groups 1, 2 and 3, respectively.

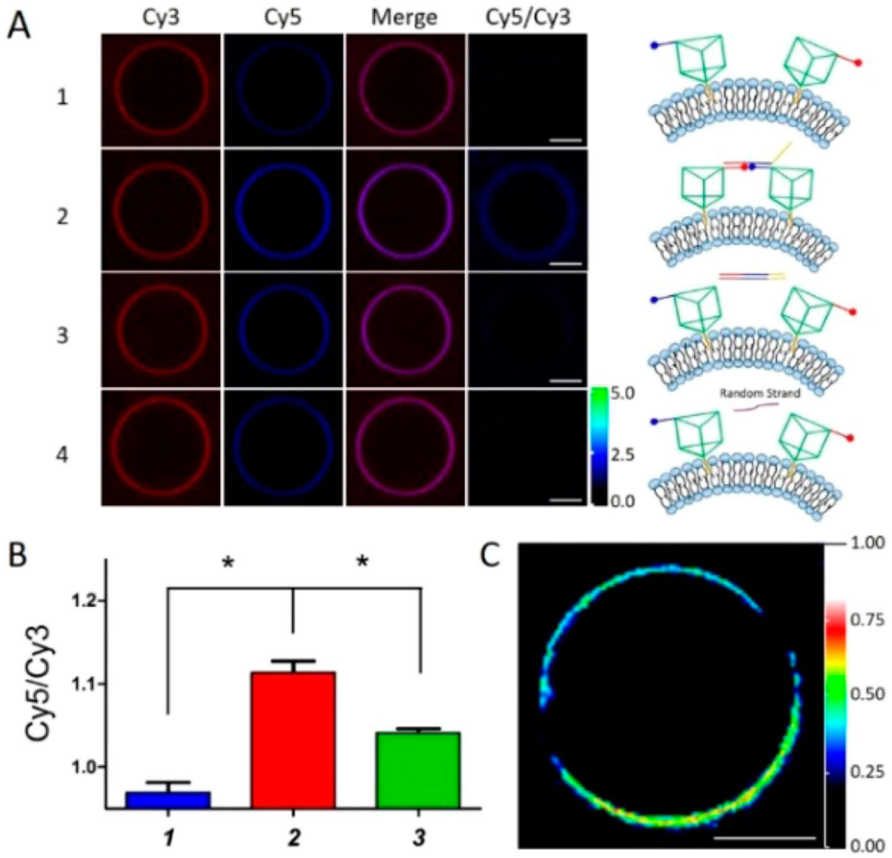

Figure 3.

Assembly/disassembly of 3D DNA nanostructures on cell-mimicking membrane of MVs. (A) Confocal laser scanning microscopy imaging of manipulation of DNA nanoprisms on MVs in 1640 medium containing 5 mM Mg^{2+} at 4 °C. (1) 500 nM TP-Cy3 and TP-Cy5. (2) Linker strand added to form dimeric nanoprism assembly of two separate TPs. (3) Displacement strand added to disassemble the dimeric nanoprism. (4) Random linker strand added to group (1) showed little effect on assembly. (B) Normalized fluorescence intensity measurements for panels 1 to 3 from panel A. Each column represents the statistical sample population of 15 MVs. *P* values were calculated by Newman–Keuls Multiple Comparison Test, $*P < 0.05$. (C) Acceptor bleaching experiment to study FRET efficiency on an individual MV. Scale bar: 5 μm.